Broadband Phase Shifter with Constant Phase Based on Negative Group Delay Circuit

Yuwei Meng, Zhongbao Wang*, Shaojun Fang, and Hongmei Liu**

Abstract—A broadband phase shifter (PS) with a constant phase based on a negative group delay (NGD) microwave circuit is proposed. The presented broadband PS is composed of distributed microstrip lines and two resistors, which is based on the positive group delay compensation principle. By tuning the electrical length of the phase shift transmission line, the constant phase can be obtained in the range of $-360° \sim 0°$. For verification, three broadband PSs with the phase shift of $-90°$, $-180°$, and $-270°$ ($90°$) are designed, fabricated, and measured at the center frequency of 1.0 GHz. The measurements show that the $-90°$ PS can achieve a constant phase of $-90° \pm 3.0°$ with a fractional bandwidth (FBW) of 73.1%; the $-180°$ PS can achieve a constant phase of $-180° \pm 5.0°$ with an FBW of 51.1%; and the $-270°$ PS can achieve a constant phase of $-270° \pm 4.0°$ with an FBW of 40.4%. Besides, the return loss is greater than 13.6 dB in the flat-phase bands.

1. INTRODUCTION

The first negative group delay (NGD) microwave circuit was proposed by Lucyszyn et al. [1], and the NGD characteristic could be obtained by RLC resonant circuit. In recent years, many novel methods for implementing NGD circuits have been proposed. The passive NGD circuits based on signal interference techniques [2] and filter theory [3] were designed. To reduce the signal attenuation, NGD circuits with active devices [4] or lossy microstrip lines [5] came into being.

With the development of NGD circuits, their applications have been more and more extensive. In [6], the NGD circuits could be used to compensate for the distortion of group delay (GD) and improve signal integrity. In addition, the NGD circuits could be used in amplifiers to improve efficiency [7]. In [8], a non-foster element was realized by the NGD circuit and has been employed in series-fed antenna arrays to compensate for the beam squint [9]. Besides, the implementation of passive devices could also base on NGD circuits, especially broadband phase shifter (PS) [10–12].

For the traditional broadband PSs, they could be divided into two categories according to the phase shift. One was the PS with a fixed phase shift [13, 14], and the other was the PS whose phase shift can be designed flexibly within a certain range [15–20]. In [15] and [16], the phase shift ranges of broadband PSs were narrow, which were $45° \sim 135°$ and $45° \sim 180°$, respectively. And the structures of the reference line must be consistent with the main line, so the design was complex. The broadband PSs could also be realized by parallel-coupled lines [17] and traditional Schiffman PS [18]. Although the broadband PSs in [17] and [18] could directly use the microstrip transmission line as the reference line, the phase shift range is still less than $180°$. Besides, the broadband PSs based on a high-pass filter [19] and modified Schiffman structure [20] have realized the phase shift range from $15°$ to $360°$ and from $0°$ to $360°$, respectively. However, the reference lines introduced in the PSs [15–20] could increase the design complexity, especially in multi-channel or multi-phase applications.

Compared with the traditional PS, the broadband PS based on the NGD circuit could realize constant phase shift without reference line [10–12]. In other words, the circuits in [10–12] had a constant and frequency-independent phase instead of a constant phase shift difference. In [10] and [11], the broadband PSs were formed by cascading an active NGD circuit and a microstrip transmission line. The active NGD circuit consisted of a field-effect transistor and a parallel RLC resonator. The ranges of phase shift in [10] and [11] were $-180° \sim 180°$ and $-180° \sim 0°$. However, there was a lack of analysis of the achievable range of phase shift, and the return loss (RL) in the band was poor. In [12], the broadband PS was designed based on the consideration of an LCL-lumped network associated with an RLC-series resonance passive NGD cell. However, only the simulation results were given. The lumped components were ideal devices, and the microstrip connection lines of the lumped devices were ignored. In addition, the broadband PSs in [11–13] were all based on lumped components, and the parasitic effect must exist. In view of this, it is necessary to propose a broadband PS based on distributed parameters transmission lines.

In this paper, a constant phase broadband PS utilizing the NGD circuit is presented to obtain a phase shift range of $-360° \sim 0°$. The proposed PS consists of distributed microstrip lines and two resistors, which is based on the positive group delay compensation principle. Details of the circuit design and both the theoretical and experimental results are given and discussed.

2. PHASE SHIFTER STRUCTURE AND DESIGN METHOD

The structure of the proposed broadband PS is shown in Fig. 1. It consists of a transmission line with characteristic impedance Z_0 and electrical length θ, whose phase slope is negative, and a well-matched NGD circuit with a positive phase slope. The total phase and GD are the sums of the TL and NGD circuit. The phase of the proposed PS is shown in Fig. 2(a). When the absolute values of the phase slope for the TL and NGD circuit are the same, the cascaded phase is a constant in the frequency band from f_1 to f_2. For GD in Fig. 2(b), in the frequency band from f_1 to f_2, the GD value of the NGD circuit is a negative constant, and the GD value of TL is a positive constant. When the absolute
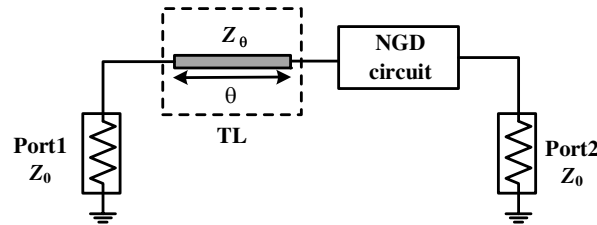
Figure 1. Structure of the proposed broadband phase shifter.
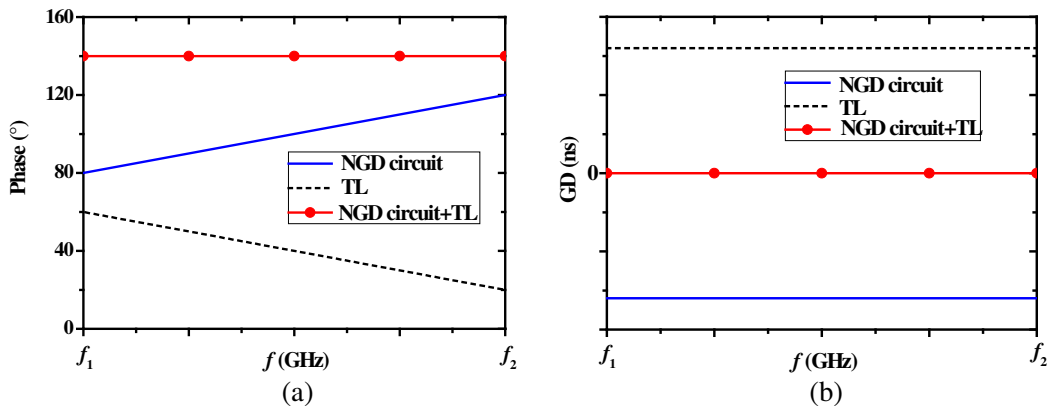
Figure 2. Ideal behaviors of the proposed broadband phase shifter. (a) Phase. (b) GD.

values of the two GD values are equal, the GD of the cascaded circuit is zero. Therefore, the NGD circuit used to compensate for the GD of TL must be a broadband NGD circuit with a flat-NGD characteristic. Compared with [21], since the characteristic impedance of the TL is Z_0 and the NGD circuit well-matched, the port matching characteristic is always well maintained during the phase shift changes. In this paper, the well-matched broadband NGD microwave circuit [22] is selected to construct the broadband PS, and the configuration is shown in Fig. 3.
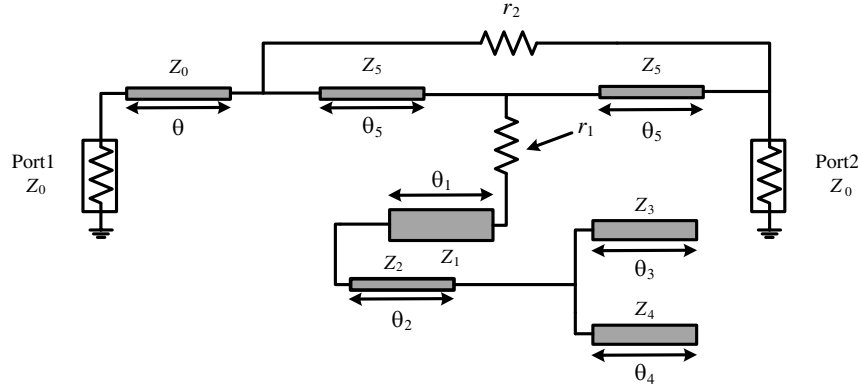
Figure 3. Configuration of the proposed broadband phase shifter.

The phase of the proposed PS can be written as

$$\tau_g = \tau_{TL} + \tau_{NGD} \tag{1}$$

The GD of TL is

$$\tau_{TL} = \theta/(2\pi f_0) \tag{2}$$

where f_0 is the center frequency.

The S_{21} of the NGD circuit is shown in Equation (3) [22].

$$S_{21}|_{f=f_0} = \frac{2\left(Z_5^2 - r_1 r_2\right) Z_0}{(r_2 + 2Z_0)\left(Z_5^2 + 2r_1 Z_0\right)} \tag{3}$$

It can be seen that the imaginary of S_{21} at f_0 is zero, so the phase is also zero. Therefore, the phase shift of the proposed PS is the phase shift of the TL. Since the GD of PS must be zero, the needed GD of the NGD circuit can be simplified as

$$\tau_{NGD} = -\theta/2\pi f_0 \tag{4}$$

Once the phase shift is determined, τ_{NGD} to be realized by broadband NGD circuit can be obtained. Then solve the parameters of the NGD circuit based on [22].

For the convenience of design, a simple procedure for the proposed PS is summarized as follows.

Step 1: Specify and determine phase shift θ at the center frequency f_0.

Step 2: Calculate τ_{NGD} with Equation (4).

Step 3: Design the NGD circuit based on [22].

Step 4: Convert all the electrical parameters to the physical dimensions based on the parameters of the substrate used, and then optimize the physical dimensions to obtain the required value and flatness of phase shift using a full-wave electromagnetic simulator.

3. PHASE SHIFT RANGE ANALYSIS

It can be seen from Equation (2) that the proposed broadband PS can realize any phase shift. For further explanation, the NGD values required for some special phase shifts in a cycle are given in Table 1.

Table 1. NGD values required for different phase shift (The unit of f_0 is GHz).

Phase Shift (°)	-45	-90	-180 (180)	-270 (90)	-315 (45)
τ_{NGD} (ns)	$-1/(8f_0)$	$-1/(4f_0)$	$-1/(2f_0)$	$-3/(4f_0)$	$-7/(8f_0)$

When f_0 is 1.0 GHz, the NGD values required to obtain the phase shift in Table 1 are -0.125 ns, -0.25 ns, -0.5 ns, -0.75 ns, and -0.875 ns, respectively. According to the τ_{NGD} in Table 1, the parameters of the NGD circuit are obtained based on the design steps in [22]. The parameters of the NGD circuit to achieve these GD values are shown in Table 2, and the GD curves are given in Fig. 4.

Table 2. Parameters of the NGD circuits required for different phase shift with $f_0 = 1$ GHz.

Phase Shift (°)	θ (rad)	r_1 (Ω)	r_2 (Ω)	Z_1 (Ω)	Z_2 (Ω)	Z_3, Z_4 (Ω)	Z_5 (Ω)
-45	$\pi/4$	188	84	94	80	24	150
-90	$\pi/2$	182	82	86	80	24	150
-180 (180)	π	167	75	68	80	24	150
-270 (90)	$3\pi/2$	140	63	54	150	24	150
-315 (45)	$7\pi/4$	115	52	30	150	24	150
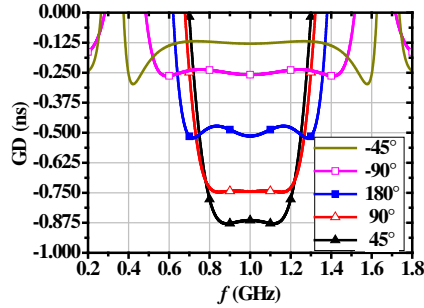
Figure 4. Curves of the required GD for different phase shift achieving by the NGD circuit.

It can be seen from Fig. 4 that as the absolute value of NGD increases, the flat bandwidth of NGD decreases. Thus, the flat-phase bandwidth decreases gradually when the phase shift of the broadband PS changes from $-360°$ to $0°$. At the same time, due to the limitation of printed circuit board technology, Z_2 cannot increase infinitely [22]. Therefore, when the NGD value is -0.125 ns, the flat-NGD characteristic cannot be realized in the frequency bands of $0.4 \sim 0.6$ GHz and $1.4 \sim 1.6$ GHz.

Figure 5 shows the phase shift curves of $-45°$, $-90°$, $180°$, $90°$, and $45°$ broadband PSs. It can be seen that the flat-phase fractional bandwidths (FBWs) are about 80%, 100%, 70%, 50%, and 40%, respectively. The flat-phase FBW of $-45°$ PS is less than that of $-90°$ PS, and the reason is that the NGD circuit used in $-45°$ PS does not reach the maximum flat-NGD bandwidth, which is consistent with the analysis in Fig. 4.

The S-parameters of the five PSs are shown in Fig. 6. It can be seen from Fig. 6(a) that the insertion loss (IL) increases during the phase shift changes from $-360°$ to $0°$. Although the broadband PS has a large attenuation, the loss can be compensated by adding a broadband amplifier to meet the application requirements. Fig. 6(b) gives $|S_{11}|$ and $|S_{22}|$. It can be seen that the proposed broadband PS can be well matched at the center frequency. It is found in Fig. 5 and Fig. 6(b) that in the flat-phase bandwidth, the RLs of the five broadband PSs are all greater than 15 dB, indicating that the broadband PS has a good impedance matching characteristic in the flat-phase bandwidth. Therefore, it can be seen from Tables 1, 2, and Figs. 4–6 that the proposed broadband PS can realize broadband phase shift function within $-360°$ to $0°$.
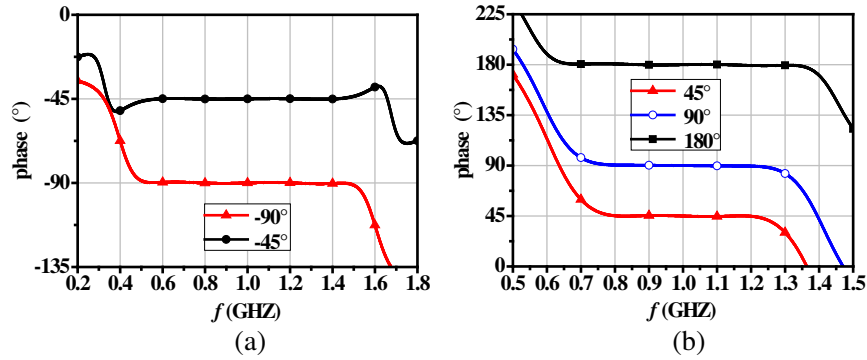
Figure 5. Phase shift curves of the proposed broadband PS. (a) Negative phase. (b) Positive phase.
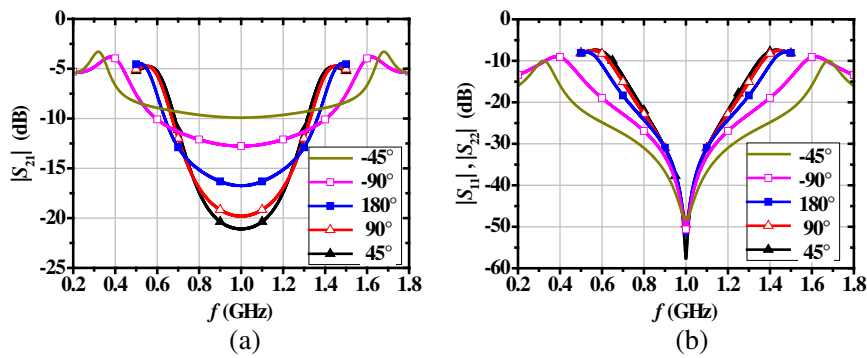
Figure 6. S-parameters of the proposed broadband PS. (a) $|S_{21}|$. (b) $|S_{11}|$ and $|S_{22}|$.

4. IMPLEMENTATION AND PERFORMANCE

To validate the design concept, three PSs are designed with the phase shift of $-90°$, $-180°$, and $-270°$ ($90°$) at center frequency $f_0 = 1\,\text{GHz}$. With the electrical parameters given in Table 2, the PSs are implemented on the substrate with a thickness of 1.5 mm, dielectric constant of 2.65, and loss tangent of 0.003. The layouts of the proposed PSs are shown in Fig. 7.
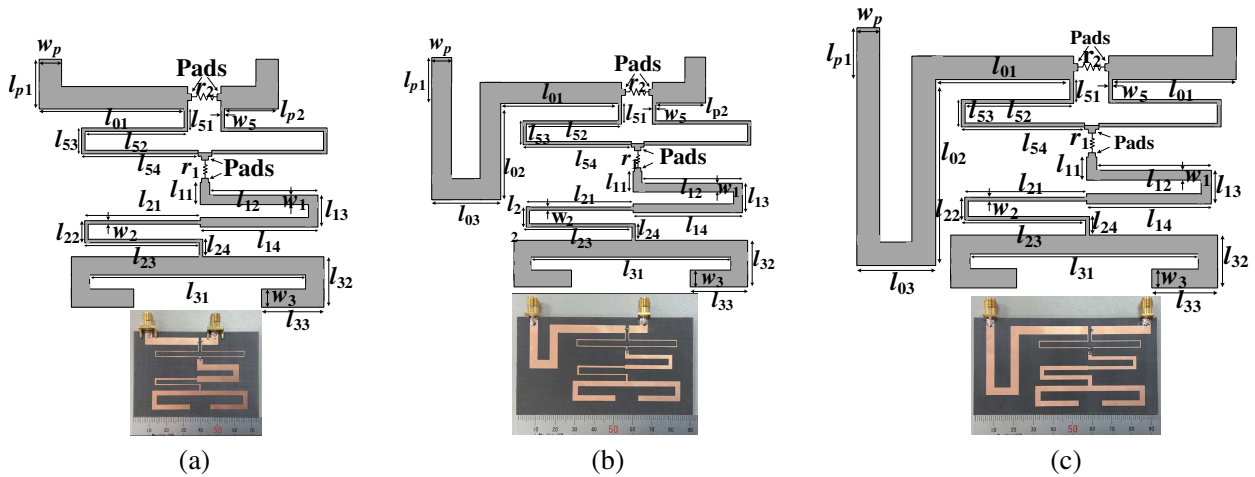
Figure 7. Layout and photograph of the proposed broadband PS. (a) $-90°$. (b) $-180°$. (c) $-270°$ ($90°$).

Using the transmission line synthesis tool *ADS Linecalc*, the physical dimensions of transmission lines are calculated without considering the discontinuous interfaces. After optimizing by HFSS EM software, the final physical dimensions are given in Table 3. Photographs of the fabricated PSs are shown in Fig. 7. The overall circuit dimensions are $51.0\,\text{mm} \times 73.5\,\text{mm}$ $(0.25\lambda_g \times 0.36\lambda_g)$, $51.0\,\text{mm} \times 91.5\,\text{mm}$ $(0.25\lambda_g \times 0.45\lambda_g)$ and $60.0\,\text{mm} \times 93.5\,\text{mm}$ $(0.29\lambda_g \times 0.46\lambda_g)$, respectively, where λ_g is the guided wavelength of 50-Ω transmission lines at the center frequency. The fabricated prototype was measured with an Agilent N5230A vector network analyzer.

Table 3. Optimized dimensions of the proposed broadband PS based on NGD microwave circuit.

Phase Shift (°)	l_{11} (mm)	l_{12} (mm)	l_{13} (mm)	l_{14} (mm)	l_{21} (mm)	l_{22} (mm)	l_{23} (mm)	l_{24} (mm)	l_{31} (mm)	
$-90°$	6.5	21.25	10.0	24.75	24.75	5.0	26.0	4.0	50.4	
$-180°$	5.0	22.75	7.0	24.75	24.75	5.0	25.25	4.0	50.4	
$-270°$ $(90°)$	4.8	22.95	6.6	24.75	24.75	7.4	24.55	5.2	50.4	
Phase Shift (°)	l_{32} (mm)	l_{33} (mm)	l_{51} (mm)	l_{52} (mm)	l_{53} (mm)	l_{54} (mm)	l_{01} (mm)	l_{02} (mm)	l_{03} (mm)	
$-90°$	10.6	22.2	3.5	25.0	3.5	25.4	31.0	-	-	
$-180°$	10.6	22.2	3.5	25.0	3.5	25.4	34.6	18.8	14.4	
$-270°$ $(90°)$	10.6	22.2	3.65	25.0	3.65	25.4	35.1	31.8	16.4	
Phase Shift (°)	l_{p1} (mm)	l_{p2} (mm)	w_1 (mm)	w_2 (mm)	w_3 (mm)	w_4 (mm)	w_5 (mm)	w_p (mm)	r_1 (Ω)	r_2 (Ω)
$-90°$	8.2	9.6	3.5	1.0	2.8	2.8	0.4	4.2	140	45
$-180°$	8.2	9.6	2.0	1.0	2.8	2.8	0.4	4.2	150	70
$-270°$ $(90°)$	8.2	-	1.8	2.2	2.8	2.8	0.4	4.2	170	70

Figures 8(a) and 9(a) compare the measured and simulated results of phase and S-parameters for $-90°$ PS. In Fig. 8(a), the measured flat-phase bandwidth $(-90° \pm 3°)$ is 851 MHz (85.0% from 572 MHz to 1432 MHz). It can be seen from Fig. 9(a) that $|S_{21}|$ is -12.8 dB at the center frequency. The IL bandwidth, which is defined as the 3-dB variation from the center frequency IL, is 813 MHz (81.0% from 662 MHz to 1435 MHz). And the input/output RL is better than 13.6 dB in the flat-phase band. In terms of phase and IL, the bandwidth of $-90°$ PS is 762 MHz (73.1% from 662 MHz to 1423 MHz). The measured and simulated results of phase and S-parameters for $-180°$ PS are shown in Figs. 8(b) and 9(b). In Fig. 8(b), the measured flat-phase bandwidth $(-180° \pm 5°)$ is 733 MHz (72.9% from 642 MHz to 1375 MHz). It can be seen from Fig. 9(b) that $|S_{21}|$ is -18.4 dB at 1 GHz. The IL bandwidth is 513 MHz (51.0% from 750 MHz to 1263 MHz). And the input/output RL is better than 14.4 dB in the flat-phase band. Figs. 8(c) and 9(c) compare the measured and simulated results of phase and S-parameters for
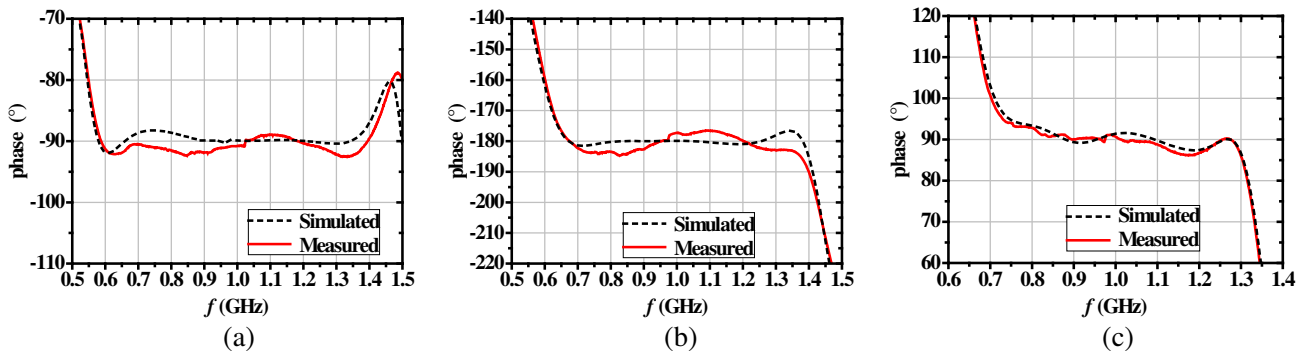
Figure 8. Simulated and measured phase of the proposed broadband PSs. (a) $-90°$. (b) $-180°$. (c) $-270°$ $(90°)$.
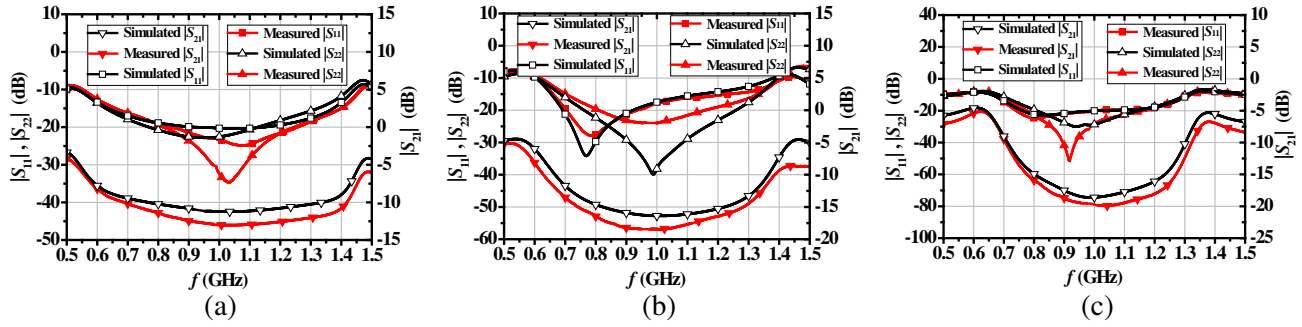
Figure 9. Simulated and measured S-parameters of the proposed broadband PSs. (a) $-90°$. (b) $-180°$. (c) $-270°$ ($90°$).

$-270°$ ($90°$) PS. In Fig. 8(c), the measured flat-phase bandwidth ($90° \pm 3°$) is $558\,\mathrm{MHz}$ (54.7% from $742\,\mathrm{MHz}$ to $1300\,\mathrm{MHz}$). It can be seen from Fig. 9(c) that $|S_{21}|$ is $-19.7\,\mathrm{dB}$ at the center frequency. The IL bandwidth is $418\,\mathrm{MHz}$ (40.4% from $825\,\mathrm{MHz}$ to $1243\,\mathrm{MHz}$). And the input/output RL is better than $15.7\,\mathrm{dB}$ in the flat-phase band.

It can be seen from Figs. 8 and 9 that the measured IL is greater than the simulation, which is mainly due to the loss of the dielectric substrate and copper conductor strip. Since the IL bandwidth of the proposed broadband PS is less than the flat-phase bandwidth, the application bandwidth of the broadband PS is equal to the IL bandwidth. In addition, there are some differences between the measured input/output RL and the simulation, which is mainly due to the differences between the actual value of the resistors and simulated models.

The comparisons of the proposed broadband PS with previous works are given in Table 4. Compared with [10, 11, 15–20], the proposed broadband PS based on the NGD microwave circuit can realize any phase shift in the range of $-360°$ to $0°$. It can be seen from phase shift bandwidth, the proposed broadband PS has greater bandwidth in the range of $-180° \sim 0°$ than that in [20]. And in the phase range of $0° \sim 180°$, the bandwidth is greater than that in [16]. Compared with [15, 17–20], although

Table 4. Comparisons between the proposed broadband PS and previous works.

References	Range of phase shift (°)	Phase shift (°)	FBW (%)	IL (dB)	RL* (dB)	Size ($\lambda_g \times \lambda_g$)
[10]	$-180 \sim 180$	90 ± 5.0	75.0	$-2 \sim 2$	8	-
[11]	$-180 \sim 0$	145 ± 10.0	160.0	$0 \sim 4$	9	0.07×0.08
[15]	$45 \sim 135$	45 ± 2.0, 60 ± 2.1, 75 ± 1, 90 ± 1.7, 105 ± 2.9, 120 ± 5.8, 135 ± 7.8	55.6	≤ 0.7	10	-
[16]	$45 \sim 180$	45 ± 1.8, 90 ± 3.0, 135 ± 3.5, 180 ± 4.2	20.7	< 2.2	13	0.35×0.25
[17]	$45 \sim 180$	180 ± 8.0	100	≤ 1.3	10	0.50×0.30
[18]	$0 \sim 180$	90 ± 2.8	58.0	< 1.1	10	0.98×0.82
[19]	$15 \sim 360$	135 ± 5.0	78.4	-	10	-
[20]	$0 \sim 360$	90 ± 3.0, 150 ± 3.0,	60.3, 51.3	< 0.97, < 0.82	19.6, 19.8	0.89×0.12, 0.88×0.10
This work	$\mathbf{-360 \sim 0}$	$\mathbf{-90 \pm 3.0}$, $\mathbf{-180 \pm 5.0}$, $\mathbf{-270(90) \pm 4.0}$	**73.1, 51.0, 40.4**	$\mathbf{-12.8 \sim -9.8}$, $\mathbf{-18.4 \sim -15.4}$, $\mathbf{-19.7 \sim -16.7}$	**13.6**	$\mathbf{0.25 \times 0.36}$, $\mathbf{0.25 \times 0.45}$, $\mathbf{0.29 \times 0.46}$

RL*: The worst RL within the flat-phase bandwidth

the bandwidth of the proposed broadband PS is narrow, the circuit size of the proposed broadband PS is smaller, and the port impedance matching performance is better. Except for [11], the proposed broadband PS has the smallest circuit size. Although the proposed broadband PS has a large IL, the IL can be compensated by adding a broadband amplifier. Besides, the low-loss NGD circuit [23] can be used to improve the IL.

5. CONCLUSIONS

In this paper, a broadband PS with a constant phase based on the NGD microwave circuit has been presented. And a simple procedure has been summarized to guide the design. The electrical length of the phase shift transmission line to obtain the constant phase in the range of $-360° \sim 0°$ has been investigated. The analysis results have shown that ideal port matching and flat-phase characteristics can be achieved. For demonstration, three broadband PSs with sizes of $0.25\lambda_g \times 0.36\lambda_g$, $0.25\lambda_g \times 0.45\lambda_g$, and $0.29\lambda_g \times 0.46\lambda_g$ have been designed, fabricated, and measured. Compared with the existing PSs, the proposed broadband PS has achieved a wider phase shift range and wider flat-phase bandwidth in the range of $-180° \sim 0°$. At the same time, the proposed PS has the advantages of small circuit size and good port impedance matching characteristics.

ACKNOWLEDGMENT

REFERENCES

1. Lucyszyn, S., I. D. Robertson, and A. H. Aghvami, "Negative group delay synthesiser," *Electron. Lett.*, Vol. 29, No. 9, 798–800, Apr. 1993.

2. Wang, Z., Y. Cao, T. Shao, S. Fang, and Y. Liu, "A negative group delay microwave circuit based on signal interference techniques," *IEEE Microw. Wireless Compon. Lett.*, Vol. 28, No. 4, 290–292, Apr. 2018.

3. Chaudhary, G., Y. Jeong, and J. Lim, "Microstrip line negative group delay filters for microwave circuits," *IEEE Trans. Microw. Theory Techn.*, Vol. 62, No. 2, 234–243, Feb. 2014.

4. Wan, F., N. Li, B. Ravelo, J. Ge, and B. Li, "Time-domain experimentation of NGD active RC-network cell," *IEEE Trans. Circuits Syst. II, Exp. Briefs*, Vol. 66, No. 4, 562–566, Apr. 2019.

5. Wan, F., N. Li, B. Ravelo, and J. Ge, "O = O shape low-loss negative group delay microstrip circuit," *IEEE Trans. Circuits Syst. II, Exp. Briefs*, Vol. 67, No. 10, 1795–1799, Oct. 2020.

6. Wan, F., X. Miao, B. Ravelo, et al., "Design of multi-scale negative group delay circuit for sensors signal time-delay cancellation," *IEEE Sens. J.*, Vol. 19, No. 19, 8951–8962, Oct. 2019.

7. Joeng, J., G. Chaudhary, and Y. Jeong, "Efficiency enhancement of cross cancellation power amplifier using negative group delay circuit," *Microw. Opt. Techn. Let.*, Vol. 61, No. 7, 1673–1677, Nov. 2019.

8. Zhang, T. and T. Yang, "A novel fully reconfigurable non foster capacitance using distributed negative group delay networks," *IEEE Access*, Vol. 7, 92768–92777, Jul. 2019.

9. Zhu, M. and C. Wu, "Reconfigurable non-foster elements and squint-free beamforming networks using active transversal filter-based negative group delay circuit," *IEEE Trans. Microw. Theory Techn.*, Vol. 70, No. 1, 222–231, Jan. 2022.

10. Ravelo, B., M. L. Roy, and André Pérennec, "Application of negative group delay active circuits to the design of broadband and constant phase shifters," *Microw. Opt. Techn. Lett.*, Vol. 50, No. 12, 3078–3080, Mar. 2008.

11. Ravelo, B., André Pérennec, and M. L. Roy, "Synthesis of frequency-independent phase shifters using negative group delay active circuit," *Int. J. RF Microwave Comput. Aided Eng.*, Vol. 21, No. 1, 17–24, Dec. 2010.

12. Nebhen, J. and B. Ravelo, "Innovative microwave design of frequency-independent passive phase shifter with LCL-network and bandpass NGD circuit," *Progress In Electromagnetics Research C*, Vol. 109, 187–203, 2021.

13. Peng, Y. and L. Sun, "A Compact broadband phase shifter based on HMSIW evanescent mode," *IEEE Microw. Wireless Compon. Lett.*, Vol. 31, No. 7, 857–860, Jul. 2021.

14. Lyu, Y. P., L. Zhu, and C. H. Cheng, "Wideband phase shifters with miniaturized size on multiple series and shunt resonators: proposal and synthetic design," *IEEE Trans. Microw. Theory Techn.*, Vol. 68, No. 12, 5221–5234, Dec. 2020.

15. Bo, W. X., Y. Z. Shao, M. P. Yong, et al., "A universal reference line-based differential phase shifter structure with simple design formulas," *IEEE Trans. Compon. Packag. Technol.*, Vol. 7, No. 1, 123–130, Dec. 2016.

16. Lyu, Y. P., L. Zhu, and C. H. Cheng, "Proposal and synthesis design of differential phase shifters with filtering function," *IEEE Trans. Microw. Theory Techn.*, Vol. 65, No. 8, 2906–2917, Aug. 2017.

17. Guo, L., H. Zhu, and A. Abbosh, "Wideband phase shifter with wide phase range using parallel coupled lines and L-shaped networks," *IEEE Microw. Wireless Compon. Lett.*, Vol. 26, No. 8, 592–594, Aug. 2016.

18. Lyu, Y. P., L. Zhu, and C. H. Cheng, "Design and analysis of Schiffman phase shifter under operation of its second phase period," *IEEE Trans. Microw. Theory Techn.*, Vol. 66, No. 7, 3263–3269, Jul. 2018.

19. Yu, X., S. Sun, X. Jing, et al., "Design of ultraflat phase shifters using multiple quarter-wavelength short-ended stubs," *IEEE Microw. Wireless Compon. Lett.*, Vol. 29, No. 4, 246–248, Apr. 2019.

20. Qiu, L. L., L. Zhu, and Y. P. Lyu, "Schiffman phase shifters with wide phase shift range under operation of first and second phase periods in a coupled line," *IEEE Trans. Microw. Theory Techn.*, Vol. 68, No. 4, 1423–1430, Apr. 2020.

21. Aboul-Seoud, A. K., A. Hamed, and A. E.-D. S. Hafez, "Wideband tunable MEMS phase shifters for radar phased array antenna," *29th Nat. Radio Sci. Conf. (NRSC)*, 593–599, Apr. 2012.

22. Meng, Y., Z. Wang, S. Fang, T. Shao, H. Liu, and Z. Chen, "Group delay flatness and bandwidth enhancement of wideband negative group delay microwave circuit," *Int. J. RF Microwave Comput. Aided Eng.*, Vol. 30, No. 12, 1–14, Sep. 2020.

23. Wang, Z., Y. Meng, S. Fang, and H. Liu, "Wideband flat negative group delay circuit with improved signal attenuation," *IEEE Trans. Circuits Syst. II, Exp. Briefs*, early access, Mar. 2022, DOI: 10.1109/TCSII.2022.3156537.